International Journal of Thermophysics, Vol. 15, No. 1, 1994

Method and Apparatus for Determination of the Total Directional Emissivity of Opaque Materials in the Temperature Range 300 to 600 K

S. X. Cheng,[1] S. X. Jing,[1] X. S. Ge,[1] and C. C. Yao[1]

Received July 8, 1993

A novel device for measurements of the normal and directional total emissivity of solid surfaces in the range 300–600 K is described. The measurements were performed using the radiation comparison method. A novel blackbody radiation source is used as a standard. The detection system consists of a pyroelectric head, a preamplifier, a chopper, and a matching lock-in amplifier with analog recorder ourput. The device is simple and well suited for routine measurements. Comparison of our results with those of previous investigations shows a good agreement.

KEY WORDS: emissometer; directional emissivity; directional total emissivity; thermal radiation.

1. INTRODUCTION

It is well recognized that the surfaces of most engineering materials exhibit some departure from diffuse behavior. Yet few data are available to enable engineers to evaluate quantitatively the variation of emissivity with direction. Furthermore, materials with specified directional emissivity or absorptivity are used in space and solar energy technologies. The heated cavity reflectometer and the device for measuring directional total emissivity, developed by Dunkle et al. [1] and Neuer and Wörner [2], respectively, can meet the needs, but they are complicated and expensive. Therefore, it seems desirable to develop a simpler device suited for routine measurements of directional total emissivity in the range 300–600 K.

[1] Department of Engineering Thermophysics, University of Science and Technology of China, Hefei, Anhui 230026, Peoples' Republic of China.

0195-928X/94/0100-0177$07.00/0

The purpose of this paper is to describe the device and its working principle and to present experimental results for several metals and nonmetals.

2. DESCRIPTION OF THE MEASUREMENT DEVICE

The radiation comparison method is used for measuring directional total emissivity. Radiances from a reference blackbody and a sample are separately measured using a pyroelectric detector system, and they are compared at the same temperature and for the same viewing conditions. The reference blackbody is a metal disk with a hemispherical reflecting shell. The sample and the metal disk are, respectively, heated with an electric heater connected to an automatic temperature control system so as to keep the same temperature between them. The components of the device are described below.

2.1. A Novel Blackbody Radiation Source

A schematic diagram of the blackbody radiation source is shown in Fig. 1. A hemispherical reflecting shell (1) with a small hole (radius r_p) at its top is situated over a disk (2) with radius r_d and emissivity ε_d, made of heavily oxidized stainless steel. The inner wall of the shell is mirror-smooth,

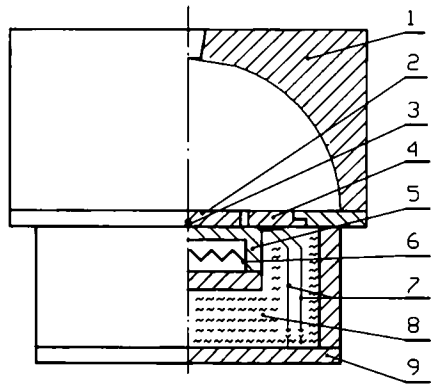

Fig. 1. Schematic diagram of a novel blackbody. (1) Hemispherical reflecting shell; (2) emitting disk; (3) thermocouple head; (4) concentric ring made of Al_2O_3 for insulation; (5) copper plate for obtaining uniform temperature of the disk; (6) electric heater; (7) thermocouple wires; (8) thermal insulation; (9) covering.

with reflectivity ρ_H and inside radius R, acting as a specular reflector. A concentric ring (4) of the disk (2) is made of Al_2O_3. The width of the gap between the ring and the disk is about 1.5 mm so as to reduce conduction losses from the disk to the ring. The disk is heated and kept at a uniform temperature, acting as a thermal emitting source. Part of the radiation emitted from the disk passes through the small aperture, and the remainder reaches the hemispheric mirror and most of it is reflected back onto the disk again. The disk absorbs part of the reflected radiation and the process is repeated.

It is assumed that (a) the hemispherical reflecting shell (1) is a specular-gray body; (b) the disk (2) and ring (4) are a diffuse-gray body; (3) when the disk (2) is heated, the ring (4) and shell (1) are, respectively, at different uniform temperatures T_d, T_r, and T_R. The theoretical analysis shows that the effective normal emissivity ε_e of the heated disk can approach 0.990, provided $r_p = 0.1R$, $r_d = 0.3R$, $\varepsilon_d \geqslant 0.80$, and $\rho_H \geqslant 0.95$. The results have also been checked by practical determination of the spectral emissive characteristics of the blackbody. The comparison gives a good agreement [3].

In comparison with the traditional heated-cavity blackbody, the advantages of the radiation source used here are that (a) it is easier to obtain a uniform temperature field over the disk, (b) no special temperature control system is needed, and (c) the construction is simpler.

2.2. Sample Holder and Heater

The geometric dimensions of the metal or nonmetal samples are as follows: diameter, 25 mm; and thickness, 3–4 mm. A schematic diagram of the sample holder and the heater is shown in Fig. 2. To keep the sample at a uniform temperature, the back surface of the sample (2) and the contact surface of the metal box (4) containing the electric heater must be polished to have a good thermal contact, and the contact area between the lid (1) and the sample (2) should be as small as possible to reduce heat losses.

The electric heater is made of a thin ceramic or a mica sheet wound with heating wire. The sample and the metal disk of the blackbody radiation source are, respectively, heated by the electric heater connected to an automatic temperature control system so as to keep the same temperature between them. Temperature measurements are performed with two pairs of the same type thermocouples (copper/constantan, 0.076 mm in diameter). The thermocouple heads are, respectively, welded on the center of the sample or disk about 0.3 mm below the measured surfaces; and the thermocouple wires are, respectively, passed through a small curved groove at the

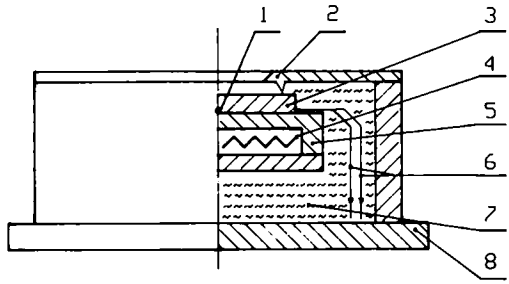

Fig. 2. Schematic diagram of the sample holder and heater. (1) Thermocouple head; (2) lid; (3) sample; (4) electric heater; (5) metal box containing electric heater; (6) thermocouple wires; (7) thermal insulation; (8) covering.

back of the sample or disk to keep a good thermal contact between the sample or disk and the heater.

2.3. Detection System

The radiation from the sample or the blackbody is separately measured using a detection system, which is composed of a pyroelectric sensor, a preamplifier, a chopper, and a lock-in amplifier with analog recorder output. The radiation absorbed by the pyroelectric crystal is converted to heat, thereby altering the lattice spacings within the crystal and causing a change in the spontaneous electric polarization of the crystal. If electrodes on the surface of the crystal are connected through an external circuit, the current generated is proportional to the rate of change of the temperature in the crystal. Thus, a modulation of the incident radiation is necessary for the operation of the detection system.

The most attractive features of the pyroelectric detector are its extremely wide spectral sensitivity and fast response. For our device, the spectral response of the pyroelectric detector is flat from 0.6 to 40 μm, the noise equivalent power is 0.5×10^{-9} W $\cdot$ Hz$^{-1/2}$, the detector area is 3.14 mm^2, the working temperature range is -20 to 40°C, and the radiant sensitivity is 2×10^6 V $\cdot$ W^{-1}. The modulation frequency of the incident radiation is 10 Hz.

2.4. Device System

A schematic of the measurement system is shown in Fig. 3. Inserting the sample holder (2) (see Fig. 2) into the support (1) with the two rota-

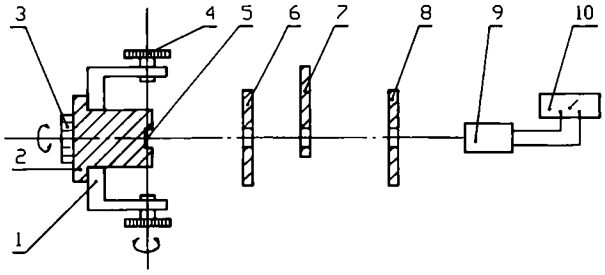

Fig. 3. Schematic of the measurement system. (1) Support; (2) sample holder; (3) axis 1; (4) axis 2; (5) sample; (6) diaphragm 1; (7) chopper; (8) diaphragm 2; (9) pyroelectric detector head and preamplifier; (10) lock-in amplifier and record.

tion axes (3 and 4) perpendicular to each other, we can revolve axis 3 or 4 to change the azimuth angle φ(0–360°) or the polar angle θ(0–75°), respectively.

Two diaphragms are set on the optical path to keep constant the solid angle subtended by the detector when viewed from the center of the sample.

Removing the sample holder from the support and substituting the blackbody for it, we can make a measurement of the blackbody radiation on the same optical path.

The aperture d_1 of the diaphragm (6) and the distance L_1 between the diaphragm (6) and the detector (9) are variable so as to select an optimum signal output. In our apparatus, $d_1 = \phi 3$–$\phi 5$ mm and $L_1 = 100$–150 mm.

3. PRINCIPLE

Figure 4 is the calculation model of the device. The energy dQ_s per unit time leaving the differential element dA_1 of the sample surface and incident on the differential element dA_2 of the detector is

$$dQ_s = I_s(\theta, \varphi, T)\, dA_1 \cos\theta dA_2/S^2 \tag{1}$$

where $I_s(\theta, \varphi, T)$ is the radiation intensity of the sample at temperature T in the direction θ, φ. The angle θ is measured from the direction normal to the surface. The angular position for $\varphi = 0$ is arbitrary. S is the distance between the center of dA_1 and dA_2, and is a constant.

Obviously, $dA_1 \cos\theta = dA$. It is just the differential element area of aperture A of the diaphragm. Because A and A_2 are constant and $A_2 \ll S^2$,

$$Q_s = [I_s(\theta, \varphi, T)/S^2] \int_A dA \int_{A_2} dA_2 = (I_s/S^2)(A)(A_2) \tag{2}$$

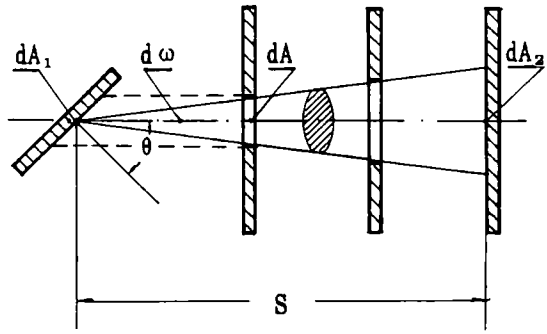

Fig. 4. Calculation model of the device. dA_1, dA_2, and dA—differential surface element of the sample, the detector, and the aperture of the diaphragm, respectively; $d\omega$—differential solid angle; θ—angle from the normal line of the sample surface; S—distance between the center of dA_1 and dA_2.

Similarly, the energy Q_b per unit time leaving the blackbody and incident upon the detector is

$$Q_b = [I_b(T)/S^2](A)(A_2) \tag{3}$$

Besides Q_s and Q_b, the environmental stray radiation Q_0 may also be received by the detector. Therefore, when the detector "sees" the sample or the blackbody, the total energy Q_{s0} or Q_{b0} received by the detector is, respectively,

$$Q_{s0} = Q_s + Q_0$$
$$Q_{b0} = Q_b + Q_0$$

Marking the output signal of the detector by S_s and S_b, responding to Q_{s0} and Q_{b0}, then

$$S_s = R[I_s(\theta, \varphi, T)(A)(A_2)/S^2 + Q_0] \tag{4}$$
$$S_b = R[I_b(A)(A_2)/S^2 + Q_0] \tag{5}$$

where R is an instrument constant.

If the detector has an output signal S_0 when neither the sample nor the blackbody is placed in the optical path, then

$$S_0 = RQ_0 \tag{6}$$

According to the definition of the directional emissivity, and from the coupled Eqs. (4)–(6), we have

$$\varepsilon(\theta, \varphi, T) = (S_s - S_0)/(S_b - S_0) \tag{7}$$

The prerequisites on which Eq. (7) is founded are that (a) the uniform temperature of the sample surface and the disk surface act as a blackbody radiation source, (b) the temperature between these two components of the apparatus is the same, and (c) the effective normal emissivity of the heated metal disk with the mirror is equal to 1. However, the practical experimental conditions deviate from the above-mentioned ideal conditions to some extent. In our apparatus, the maximum radial temperature nonuniformity of the sample or the disk surface is less than 1.5 or 0.5 K, respectively, when the surface temperature is at 600 K. The maximum temperature difference between these two components of the apparatus can approach within 1.5 K using an automatic temperature control system with a precision of 0.5 K. The shape of the radiation source emitting from the sample is changed from a circle, 4 mm in diameter, to an ellipsoid, 16 mm in major axis and 4 mm in minor axis, as the angle θ of viewing increases from 0 to 75°. The test showed that neither the maximum temperature nonuniformity nor the maximum temperature difference between the two components of the apparatus increases with increasing θ. Moreover, the aperture of the diaphragm plays a very important role in keeping the solid angle constant and optimizing the radiance reaching the detector. Therefore, as the viewing angle increases, the radiance reaching the detector is related according to Eq. (7).

4. RESULTS AND DISCUSSION

4.1. Normal Total Emissivity of Several Metals and Nonmetals

In order to check the reliability of the device, the normal total emissivity of a heavily oxidized stainless steel was measured by our device

Table I. The Normal Total Emissivity of a Heavily Oxidized Stainless Steel (at $T = 600$ K)[a]

	i								
	1	2	3	4	5	6	7	8	9
ε_i (%)	79.4	77.9	77.9	79.4	77.6	77.4	79.2	78.6	78.0
ε_n (%)					78.4				
σ					7.44×10^{-3}				

[a] i, test run number; ε_i, experimental results; ε_n average value of ε_i; σ standard error.

Table II. Comparison of the Normal Emissivity of Some Surfaces with the Results of Previous Work

Material	Surface appearance	Measurement		Literature		Ref. No.
		T(K)	ε_n(%)	T(K)	ε_n(%)	
Gold	Highly polished	403	2.08	403	1.8	5
Copper	Lightly oxidized	323	3.92	313	3.7	6
		343	4.00			
Aluminum	Polished	373	4.00	323–773	4.0–6.0	7
Stainless steel	Clean	343	20.0	300–1000	22.0–35.0	8
Plain paper		373	91.7	368	92.0	6
SiC		373	93.3	373	93.0	9
Copper	Heavily oxidized	373	78.2	311	78.0	6
Skin	Palm	307	94.7	308	95.0	9
				300	95.0	8

and by an apparatus offered by the China National Bureau of Standards [4]. The experimental results for our device are listed in Table I. It shows that the repeatability of the measured values is satisfactory and the maximum relative error, comparing our result of 0.784 with the national standard value of 0.799, is less than 2%. Some experimental results are listed in Table II and compared with those of the previous works; they show a good agreement.

4.2. Directional Total Emissivity for Some Nonmetals

The measurement results of the directional total emissivity for the heavily oxidized surface of copper and stainless steel, SiC surface, and plain paper are shown in Fig. 5. The results show that the emissivity is almost constant for $\theta < 55^\circ$ and for $55^\circ \leqslant \theta \leqslant 75^\circ$, the total emissivity decreases with increasing θ, and they are independent of angle φ. The results are in agreement with those in Ref. 6.

4.3. Influence of Surface Roughness on $\varepsilon(\theta, \varphi, T)$

Figure 6 shows the directional total emissivity for a polished surface of aluminum and a surface with mechanically fabricated V-grooves on the polished surface. The results show the following. (a) A behavior typical of polished metals in directional emissivity tends to increase with increasing angles of emission, and there is no dependence on the angle φ. This was predicted by the electromagnetic theory long ago. (b) The directional total

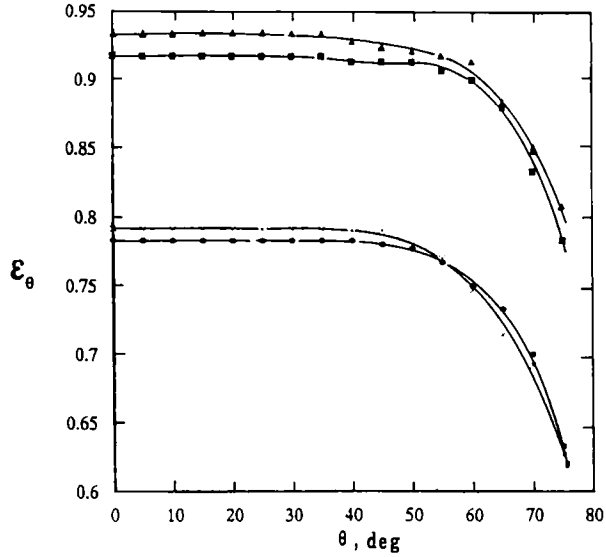

Fig. 5. Angular distribution of the emissivity of some non-metallic materials: (▲) SiC; (×) heavily oxidized stainless steel; (■) plain paper; (●) heavily oxidized copper.

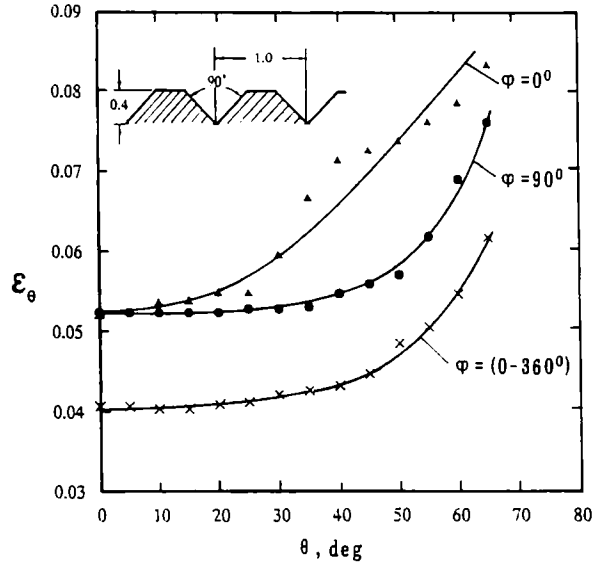

Fig. 6. Influence of surface roughness and φ on ε_θ: (×) polished surface of aluminum; (▲) mechanical V-grooves on the polished surface at $\varphi = 0°$; (●) mechanical V-grooves on the polished surface at $\varphi = 90°$.

emissivity of the rough surface with regular V-grooves of 90° angle running parallel to each other is greater than that of the polished surface and has a nonisotropic behavior at the surface.

5. ERROR ANALYSIS

In fact, in our apparatus, the maximum radial nonuniform temperature of the sample or disk surface, as indicated in Section 3, is so small (1.5/600) that the nonuniformity can be neglected. The output signal S_0 can also be zeroed in the recorder due to the weak signal. Therefore, a formula for estimating the error of the method can be expressed as

$$(\delta\varepsilon/\varepsilon)^2 \leqslant (\delta S_s/S_s)^2 + (\delta S_b/S_b)^2 + (\delta\varepsilon_b/\varepsilon_b)^2 + 2(4\Delta T/T)^2 \tag{8}$$

Apparently, the first two terms on the right-hand side of Eq. (8) express the measurement errors of the output signal, S_s or S_b, respectively. The last two terms are, respectively, the errors due to the deviation of our blackbody from ideal conditions or the sample surface temperature from the reference blackbody temperature.

For a heavily oxidized stainless steel at $T = 600$ K, $\theta = 0°$, and $\varphi = 0°$, we have

$$\delta S_s/S_s = 1/655, \qquad \delta S/S_b = 1/845, \qquad \delta\varepsilon_b/\varepsilon_b = 0.04$$

(taken from Ref. 3), and $\Delta T/T = 2.0/600$

so $\delta\varepsilon/\varepsilon \leqslant 0.045$.

For a highly polished gold at $T = 403$ K, $\theta = 0°$, and $\varphi = 0°$, we have

$$\delta S_s/S_s = 1/11, \qquad \delta S_b/S_b = 1/470, \qquad \delta\varepsilon_b/\varepsilon_b = 0.04$$

(taken from Ref. 3), and $\Delta T/T = 2.0/403$

so $\delta\varepsilon/\varepsilon \leqslant 0.10$.

Obviously, for the sample with a high emissivity, the major source of error is $\delta\varepsilon_b/\varepsilon_b$, and for the sample with a low emissivity, the errors result mainly from $\delta S_s/S_s$ and $\delta\varepsilon_b/\varepsilon_b$.

6. CONCLUSIONS

The test apparatus described here is well suited for routine measurements of the normal and directional total emissivity of solid surfaces in the range 300–600 K. It is very simple to operate and has a high precision. Comparison of our results with previous work given by other investigators

indicates a good agreement. The machining and grinding of metals can lead to a dramatic effect, resulting in a increase in emissivity. Thus, a surface with a directional selectivity of radiation can be obtained; this kind of surface is useful in applications related to solar energy and space technology.

REFERENCES

1. R. V. Dunkle, D. K. Edwards, J. T. Gier, K. E. Nelson, and R. D. Roddick, in *Progress in International Research on Thermodynamic and Transport Properties* (Princeton Press, Princeton, NJ, 1962), pp. 541–598.
2. G. Neuer and B. Wörner, *Proceedings of the 7th Symposium on Thermophysical Properties*, A. Cezairliyan, ed. (Am. Soc. Mech. Eng., New York, 1977), pp. 250–255.
3. C. C. Yao, X. S. Ge, and S. X. Cheng, *J. Eng. Thermophys. China* **12**:164 (1991) (in Chinese).
4. Q. T. Xu, R. H. Fu, and Y. Fei, *China National Standard, GB7286.1-7286.2-87* (1987) (in Chinese).
5. E. R. G. Eckert and R. M. Drake, Jr., *Introduction to the Transfer of Heat and Mass* (McGraw-Hill, New York, 1959), pp. 529–530.
6. E. M. Sparrow and R. D. Cess, *Radiation Heat Transfer* (McGraw-Hill, New York, 1978), pp. 55–56.
7. S. M. Yang, *Heat Transfer* (People Education Press, Beijing, 1983) (in Chinese).
8. F. P. Incropera and D. P. DeWitt, *Fundamentals of Heat Transfer* (Wiley, New York, 1981).
9. Y. Q. Luo, M.S. thesis (University of Science and Technology of China, 1988) (in Chinese).

Printed in Belgium
Verantwoordelijke uitgever:
Hubert Van Maele
Altenastraat 20 B-8310 St.-Kruis